

## **Tin selenide thin films prepared through combination of chemical precipitation and vacuum evaporation technique**

ZULKARNAIN ZAINAL<sup>1\*</sup>, SARAVANAN NAGALINGAM<sup>1</sup>, ANUAR KASSIM<sup>1</sup>,  
MOHD. ZOBIR HUSSEIN<sup>1</sup>, WAN MAHMOOD MAT YUNUS<sup>2</sup>

<sup>1</sup>Department of Chemistry, Universiti Putra Malaysia, 43400 Serdang, Selangor, Malaysia

<sup>2</sup>Department of Physics, Universiti Putra Malaysia, 43400 Serdang, Selangor, Malaysia

Tin selenide thin films were prepared through combination of chemical precipitation and vacuum evaporation technique. The vacuum deposition was carried out using different quantities of the starting material. The differences in the structural and compositional properties of the films deposited were studied. The films were characterised using various techniques such as X-ray diffractometry, scanning electron microscope and energy dispersive analysis of X-ray. Photoactivity of the samples was studied using the linear sweep voltammetry. The films were found to be p-type semiconductors. The optical bandgap energy was found to be indirect and equal to  $E_g = 1.25$  eV.

Key words: *tin selenide; photoelectrochemical cell; thin film; evaporation*

### **1. Introduction**

The search for thin-film materials for solar energy conversion and other related applications has been recently identified. It is not surprising now that a lot of effort has been geared towards metal chalcogenides as this class of materials had shown somewhat superior performance when compared to others [1, 2]. The synthesis and characterisation of metal chalcogenides via different techniques have attracted considerable attention due to their application prospects. These compounds are also reported to be used as sensor and laser materials, thin films polarizers and thermoelectric cooling materials [1, 2]. They are usually prepared through electrochemical and chemical deposition method and are quite attractive for designing systems for

---

\*Corresponding author, e-mail: [zulkar@fsas.upm.edu.my](mailto:zulkar@fsas.upm.edu.my).

electro-optics and photoelectrochemical (PEC) solar cells. Improvements in process reproducibility laid the groundwork for introducing a new product, which is composed of several innovative materials and methods. These metal chalcogenides have been prepared in the form of thin films by various researchers.

A considerable attention has also been given by various researchers to the preparation techniques of tin selenide (SnSe) thin films. Among the methods used are chemical bath deposition [3], vacuum evaporation, chemical vapour deposition [4–12] and electrodeposition [13, 14]. SnSe is a narrow band gap binary IV–VI semiconductor displaying a variety of applications such as an essential material in photoelectrochemical solar cells to suppress the photocorrosion and to enhance the fill factor in electrical switches and in junction devices [12]. Because of their anisotropic character, tin chalcogenides are attractive layered compounds, and can be used as cathode materials in lithium intercalation batteries [15]. The indirect character of the bandgap of SnSe is a common property of IV–VI compounds and has been confirmed by band structure calculations for SnSe [16]. It has orthorhombic crystal structure with layers stacked along the  $c$  axis and  $a = 4.30$  Å,  $b = 4.05$  Å and  $c = 11.62$  Å [17]. Motivated by the potential applications of tin chalcogenides, investigations of these compounds are becoming particularly active in the field of materials chemistry. The studies comprise spectroscopy, sensing properties and electronic structure of SnSe compounds [18]. In the present work, we have prepared SnSe thin films through vacuum evaporation. The SnSe source for the evaporation was obtained through chemical precipitation technique.

## 2. Experimental

SnSe powder was obtained by the chemical synthesis. The desired amount of elemental selenium was dissolved in 5.6 M NaOH solution and stirred rapidly for 20 min. Upon complete dissolution of elemental Se, the Sn solution complexed with EDTA was added and the stirring process was maintained for almost 15 min. Black precipitate (SnSe) obtained was filtered and washed with distilled water and dried in oven for 6 h. The required amount of the SnSe powder was used as the source for the vacuum evaporation system to obtain two samples of SnSe films with different thicknesses.

Thin films of SnSe were deposited using the synthesised powder in an Edwards Auto 306 Vacuum Coating Unit. Indium-doped tin oxide (ITO) glass was used as the substrate. The substrates were cleaned ultrasonically in ethanol and distilled water before the deposition process. The vacuum was kept at  $8 \times 10^{-5}$  mbar. SnSe powder was evaporated from a tungsten filament onto the ITO glass substrate to form the semiconductor layer. The source-to-substrate distance was maintained at 15 cm. The films were found to be uniform, free of pinholes and adhered well to the ITO glass substrate, their thicknesses amounted to 10 and 22 µm.

X-ray diffraction (XRD) analysis was carried out using a Siemens D-5000 Diffractometer for the  $2\theta$  ranging from  $2^\circ$  to  $60^\circ$  with  $\text{CuK}_\alpha$  line used as a beam ( $\lambda =$

1.5418 Å). Scanning electron microscopy (SEM) and energy dispersive analysis of X-ray (EDX) was performed on a JEOL JSM 6400 Scanning Microscope. Optical absorption study was carried out using the Perkin Elmer UV/Vis Lambda 20 Spectrophotometer. The film-coated ITO glass was placed across the sample radiation pathway while an uncoated ITO glass was put across the reference path. From the analyses of the absorption spectra the band gap energy  $E_g$  was determined. The ellipsometry technique was used to determine the thickness of the films using an ELX-02C Ellipsometer.

Photoelectrochemical (PEC) experiments were performed in the  $[\text{Fe}(\text{CN})_6]^{3-}/[\text{Fe}(\text{CN})_6]^{4-}$  redox system, by running linear sweep voltammetry (LSV) between  $-0.4$  V and  $-1.0$  V. The electrolytes were prepared using analytical grade reagents and deionised distilled water. An EG&G Princeton Applied Research potentiostat driven by a software model 270 Electrochemical Analysis System was used to control the LSV process and to monitor the current and voltage profiles in a conventional three-electrode cell. Ag/AgCl was used as the reference electrode. The working and counter electrodes were made of SnSe coated ITO glass substrate and platinum, respectively. The counter electrode was polished prior to the insertion into the electrolyte cell. A tungsten-halogen lamp (100 W) was used for illuminating the electrode.

### 3. Results and discussion

The XRD of the SnSe powder obtained from the chemical precipitation technique is shown in Fig. 1. The peaks in the pattern indicate the formation of the orthorhombic phase of SnSe. The results are well matched with the standard JCPDS values (File No. 32-1382) for SnSe (Table 1). No peaks corresponding to Se in the XRD pattern are seen. This indicates that the sample powder contains no elemental Se.

Table 1. XRD data of SnSe powder

$2\theta$ (deg)	$d$ (Å)	
	Values obtained	JCPDS values (File No. 32-1382)
25.2	3.53	3.52
29.3	3.04	3.05
30.2	2.94	2.94
31.0	2.90	2.90
37.5	2.39	2.38
43.0	2.09	2.09
49.3	1.84	1.83
53.9	1.69	1.68

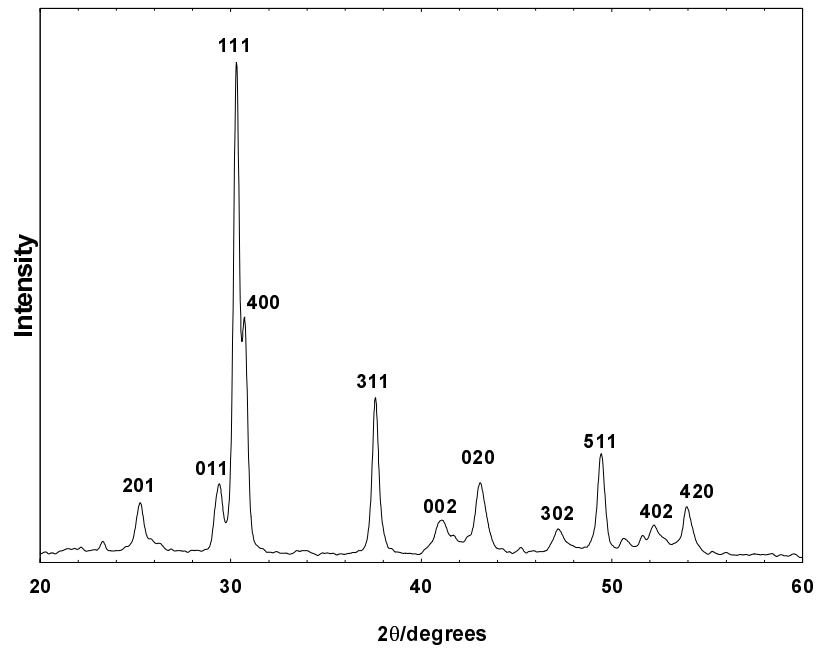


Fig. 1 X-ray diffraction spectrum of SnSe powder

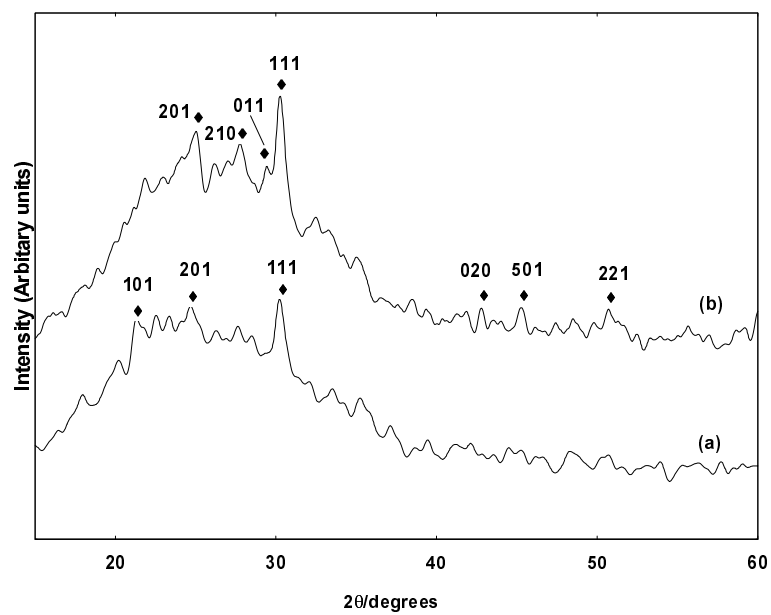


Fig. 2 X-ray diffraction spectrum of SnSe thin films with different thicknesses: a) 0.10 μm, b) 0.22 μm

The XRD patterns of vacuum-deposited SnSe thin films having thickness 0.10  $\mu\text{m}$  and 0.22  $\mu\text{m}$  are shown in Fig. 2a, b, respectively. The broad peak appearing at low angle is due to the glass substrate itself. The observation of X-ray peaks in both SnSe thin films indicates that the vacuum-deposited films are polycrystalline. The intensities of the signals are rather weak due to the thin film nature of the samples. Table 2 lists the observed  $d$ -values for SnSe thin films in comparison with the JCPDS standard data (File No. 32-1382). The observed  $d$ -values are in a good agreement with the standard values for the orthorhombic structure of SnSe. The strongest peak for both films occurred at  $2\theta = 30.3^\circ$  with  $d = 2.95 \text{ \AA}$  (corresponding to the (111) reflection). It indicates that the preferred orientation lies along the (111) direction for vacuum deposited SnSe thin films.

Table 2. XRD data of SnSe films

Thickness ( $\mu\text{m}$ )	$2\theta$ (deg)	$d$ ( $\text{\AA}$ ) measured	$d$ ( $\text{\AA}$ ) standard (File No. 32-1382)	$hkl$
0.10	21.3	4.16	4.15	101
	24.7	3.60	3.52	201
	30.2	2.95	2.95	111
0.22	25.1	3.54	3.52	201
	27.7	3.31	3.37	210
	29.3	3.04	3.05	011
	30.3	2.95	2.95	111
	42.8	2.11	2.10	020
	45.2	2.00	2.03	501
	50.6	1.80	1.80	221

The dominant orientation in the (111) plane has also been reported by other researchers for the SnSe thin films deposited by vacuum deposition [12, 17, 19, 20] and electrochemical deposition [4, 13, 21]. As expected, the crystallinity of the thicker film is better and more X-ray peaks are observed. The intensity of the (111) peak shows a significant increase as the thickness of the SnSe film increases. The crystallite sizes (grain diameter)  $D$  of the deposits were determined using the Scherrer's formula [17]:

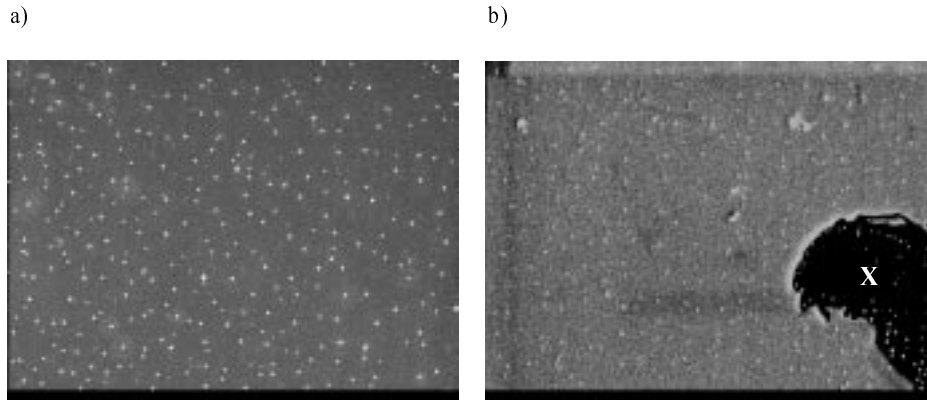
$$D = \frac{K\lambda}{\omega \cos \theta}$$

where  $\lambda$  is the wavelength of X-rays,  $\theta$  the Bragg angle and  $\omega$  the full width at a half maximum (in radians).  $K$  varies with ( $hkl$ ) and crystallite shape but usually is nearly equal to 1. The grain size increased from 14.3 nm to 15.0 nm when the thickness of the film was increased (see Table 3).

Table 3. Grain size in SnSe thin films

Thickness ( $\mu\text{m}$ )	Peak	Grain size (nm)
0.10	111	14.3
0.22	111	15.0

Figure 3 shows the SEM micrographs of SnSe films. The thinner films exhibit growth of small grains distributed across the surface of the substrate. To have a visual reference on the two films and to be able to compare them, a small portion of the substrate surface containing the thicker film was cleaned with  $\text{HNO}_3$ . This portion of the surface is marked with 'X' in Fig. 3b. This reveals the thicker surface coverage of the SnSe onto the substrate in the latter film. The micrographs of these films indicate uniform surface coverage and smooth SnSe texture. The EDX analysis indicates the Sn to Se ratio to be 0.9, which is almost at the stoichiometry level.

Fig. 3. SEM micrographs of SnSe prepared at different thickness: (a) 0.10  $\mu\text{m}$  (b) 0.22  $\mu\text{m}$ 

The band-gap energy and transition type was derived from mathematical treatment of the data obtained from the optical absorbance vs. wavelength with the following relationship for near-edge absorption:

$$A = \frac{k(h\nu - E_g)^{n/2}}{h\nu}$$

where  $\nu$  is the frequency,  $h$  is the Planck's constant,  $k$  equals a constant while  $n$  carries the value of either 1 or 4. Figure 4 shows the absorbance spectra of the films of different thicknesses. It is clear that the thicker film has a higher absorption. This could be due to more SnSe material deposited onto the surface of the substrate. The band gap  $E_g$  could be obtained from a straight line plot of  $(Ah\nu)^{2/n}$  as a function of  $h\nu$ : an extrapolation of the value of  $(Ah\nu)^{2/n}$  to zero, will give  $E_g$ . If a straight line graph is

obtained for  $n = 1$ , it indicates a direct electron transition between the states of the semiconductor, whereas the transition is indirect if a straight line graph is obtained for  $n = 4$ .

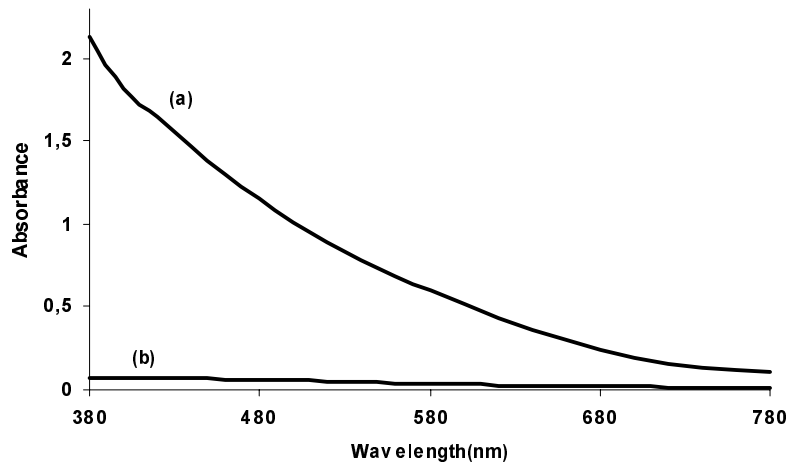


Fig. 4. Optical absorbance vs. wavelength spectrum for SnSe films. Thickness: a) 0.22  $\mu\text{m}$ , b) 0.10  $\mu\text{m}$

A linear trend is apparent where  $n$  in the relationship (1) equals 4. The straight-line behaviour in Fig. 5 testifies an indirect transition of the band structure. The line segments required to by pass the energy of the gap lies at about 1.25 eV for the SnSe film. A similar band-gap value has also been reported by other researchers for vacuum evaporated SnSe films [6, 17, 19, 20].

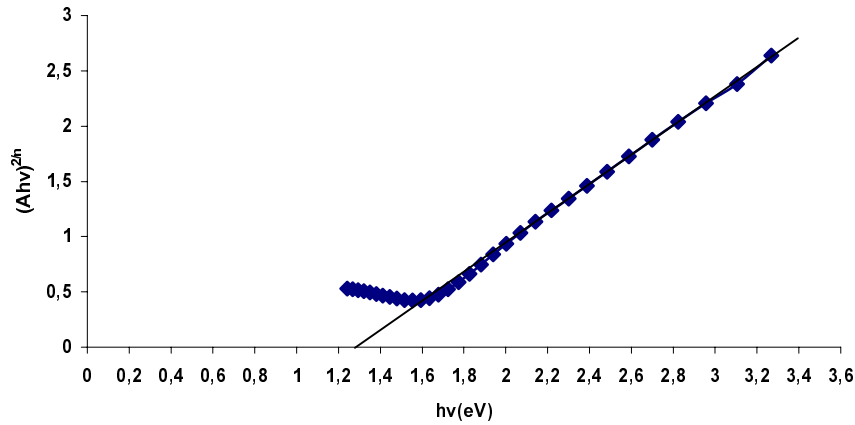


Fig. 5. Plot of  $(Ahv)^{2n}$  vs.  $h\nu$  in an SnSe film with  $n = 4$

Figure 6 shows the difference between the photocurrent  $I_p$  and the dark current  $I_d$  for the two films when illuminated with a tungsten-halogen lamp (100 W). An in-

crease in the current could be observed for the both samples, which was employed as a cathode in the electrochemical cell as the potential is swept to more negative region. A comparison between the two samples indicates an increase in the photoresponse for the thicker film. The reason for the increase in the photoresponse could be explained in term of the grain size. As the grain size increases from 14.3 to 15.0 nm, the grain boundaries are reduced. The boundaries are known to act as recombination centres for minority carriers and trapping centres for majority carriers.

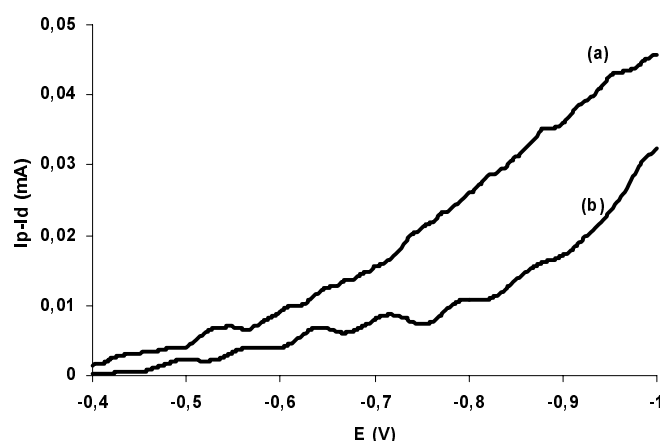


Fig. 6. Comparison of photosensitivity of the samples. Thickness (a) 0.22  $\mu\text{m}$  (b) 0.10  $\mu\text{m}$

The dependence shown in Fig. 6 confirms that the films possess semiconducting behaviour. The fact that the photocurrent occur on the negative (cathode) potential indicates that the films prepared are of the *p*-type and they can be deployed as photo cathode in the photoelectrochemical cell application to facilitate a reduction reaction of the electro active species in the solution.

#### 4. Conclusion

Clear, transparent SnSe films with different thickness could conveniently be prepared by combination of chemical precipitation and vacuum evaporation technique. The SnSe powder preparation method is less tedious than the previously used solid-state method [6, 17, 19, 20]. The preferred orientation of the crystallites lies along the (111) direction. The thicker SnSe film exhibits a higher photoactivity. The band gap was found to be indirect and equal to 1.25 eV.

#### Acknowledgements

We are grateful to the Malaysian Government for providing the grant under IRPA No. 09-02-04-0369-EA001. We would like to thank the Department of Physics, Universiti Putra Malaysia for providing



the laboratory facilities. One of us (S.N.) would like to thank the Ministry of Science, Technology and the Environment for the National Science Fellowship (NSF).

### References

- [1] LINDGREN T., LARSSON M., LINDQUIST S., Sol. Energy Mater. Sol. Cells, 73 (2002), 377.
- [2] ZWEIBEL K., Sol. Energy Mat. Sol. Cells, 63 (2000), 375.
- [3] PRAMANIK P., BHATTACHARYA S., J. Mater. Sci. Lett., 7 (1988), 1305.
- [4] JOHN J., PRADEEP B., MATHAI E., J. Mater. Sci., 29 (1994), 1581.
- [5] BENNOUNA A., TESSIER P., PRIOL M., DANG TRAN Q., ROBIN S., phys. stat. sol. (b), 117 (1983), 51.
- [6] DANG TRAN Q., phys. stat. sol. (a), 86 (1984), 421.
- [7] RAO T.S., CHAUDHURI A.K., J. Phys. D: Appl. Phys., 18 (1985), L35.
- [8] RAO T.S., SAMANTHARY B.K., CHAUDHURI A.K., J. Mater. Sci. Lett., 4 (1985), 743.
- [9] DANG TRAN Q., Thin Solid Films, 149 (1987), 197.
- [10] SHARON M., BASAVASWARAN K., Solar Cells, 20 (1987), 323.
- [11] SINGH J.P., BEDI R.K., Jap. J. Appl. Phys., 29, 6 (1990), L869.
- [12] SUGUNA P., MANGALARAJ D., NARAYANDASS S.A.K., MEENA P., phys. stat. sol. (a), 155 (1996), 405.
- [13] SUBRAMANIAN B., MAHALINGAM T., SANJEEVIRAJA C., JAYACHANDRAN M., CHOCKALINGAM M.J., Thin Solid Films, 357 (1999), 119.
- [14] ENGELKEN R.D., BERRY A.K., VAN DOREN T.P., BOONE J.L., SHAHNAZARY A., J. Electrochem. Soc., 133 (1986), 581.
- [15] YAMAKI J., YAMAJI A., Physica, B 150 (1981), 466.
- [16] SINGH J.P., BEDI R.K., Thin Solid Films 199 (1991), 9.
- [17] PADIYAN D.P., MARIKANI A., MURALI K.R., Cryst. Res. Technol. 35 (2000), 949.
- [18] AGARWAL A., J. Cryst. Growth, 183 (1998), 347.
- [19] SOLIMAN H.S., ABDEL HADY D.A., ABDEL RAHMAN K.F., YOUSSEF S.B., EL-SHAZLY A.A., Physica A, 216 (1995), 77.
- [20] SINGH J.P., BEDI R.K., J. Appl. Phys., 68, 6 (1990), 2776.
- [21] ZAINAL Z., SARAVANAN N., ANUAR K., HUSSEIN M.Z., YUNUS W.M.M., Greenwich J. Sci. Tech. (in press).

*Received 21 January 2003*

*Revised 14 March 2003*